



## Effect of $\text{Na}_2\text{CO}_3$ on reduction and melting separation of ludwigite/coal composite pellet and property of boron-rich slag

Guang WANG, Qing-guo XUE, Jing-song WANG

State Key Laboratory of Advanced Metallurgy, University of Science and Technology Beijing, Beijing 100083, China

Received 31 January 2015; accepted 21 July 2015

**Abstract:** The effects of  $\text{Na}_2\text{CO}_3$  on the reduction and melting separation behavior of ludwigite/coal composite pellet, the desulfurization ratio and the property of the separated boron-rich slag were investigated at laboratory scale in the present work.  $\text{Na}_2\text{CO}_3$  could improve the reduction rate of the composite pellet to some extent. The melting separation of the composite pellet became increasingly difficult with the increase of  $\text{Na}_2\text{CO}_3$  in the pellet due to the sharply increasing of the melting point of slag. The sulfur content of the iron nugget gradually decreased from 0.27% to 0.084% (mass fraction) with the  $\text{Na}_2\text{CO}_3$  content in the pellet increasing from 0 to 6%. The efficiency of extraction of boron (EEB) of the slow cooled boron-rich slag decreased from 86.46% to 59.52% synchronously.  $\text{Na}_2\text{CO}_3$  had obviously negative effect on melting separation of the composite pellet and boron extraction of the boron-rich slag.

**Key words:** ludwigite; carbon composite pellet; reduction and melting separation; desulfurization; boron-rich slag; boron extraction

### 1 Introduction

Boron compounds, chiefly borates, are commercially important and there are more than 300 end uses for borates. World consumption of borates was projected to reach  $2.0 \times 10^6$  t of  $\text{B}_2\text{O}_3$  by 2014, compared with  $1.5 \times 10^6$  t of  $\text{B}_2\text{O}_3$  in the year of 2010. China makes an important contribution to the increase of the total boron consumption in the world due to its large demand [1]. Boron resource of China is rich in total amount and ranks the fifth in the world. However, most of the boron mineral resources in China are of low grade. With the depletion of the traditional high grade szaibelyite ore and increasing demand for boron products, comprehensive utilization of the domestic low grade boron resources becomes the main task presented before the Chinese boron industry to guarantee a sustainable development. Fortunately, there are  $2.8 \times 10^8$  t of low grade ludwigite deposits in Liaoning and Jilin Provinces, which account for 57.88% boron reserves and 1% iron reserves in China and are regarded as the main alternate resource of szaibelyite ore [2].

Ludwigite is a kind of complex iron ore, which is rich in the elements of iron, boron and magnesium. The

key factors in the comprehensive utilization of the ludwigite resource are the high separation degree of boron and iron elements, and high yield and good quality of the separated products. Many Chinese researchers have made lots of contribution to the mineralogy and utilization of the promising resource [3–6]. The ore has very complicated mineral phase compositions and the iron containing minerals finely embed with the boron containing minerals and other gangue minerals. Therefore, it is too difficult to realize high separation degree of boron and iron through traditional ore dressing method. A novel process of comprehensive utilization of ludwigite by carbon composite pellet reduction and melting separation technology, i.e., the iron nugget technology, has been proposed by WANG et al [7–9]. The so-called boron-containing iron nugget and boron-rich slag can be obtained in the new process. The boron-containing iron nugget may be used as raw material of steelmaking and boron-rich slag may be used as raw material of boron industry. The new process has the merits of coke free, short flow sheet, high separation degree of boron and iron, high boron content in the boron-rich slag, etc.

Although the MgO content in the slag is more than 50% (mass fraction), the desulfurization ability of the

slag is not good enough in the new process and nearly about 56% of the total sulfur in the pellet repartitions into the iron nugget. So, new desulfurizing agent of high efficiency should be introduced into the pellet. Sodium carbonate ( $\text{Na}_2\text{CO}_3$ ) is widely used as the desulfurizing agent in the metallurgical process, which has high desulfurization efficiency [10]. However, the extraction property of boron element of the boron-rich slag is the most important in the utilization of ludwigite. The iron and slag melting separation of the ludwigite/coal composite pellet is the premise of the new process proposed by the authors. Based on the above analysis, the effect of  $\text{Na}_2\text{CO}_3$  on the reduction and melting separation behaviors of the ludwigite/coal carbon composite pellet and the properties of iron nugget and boron-rich slag were studied in the present work. A further understanding of the mechanism of the new process could be obtained from the present experimental results.

## 2 Experimental

### 2.1 Raw materials

The ludwigite iron concentrate used in the present study is obtained from Dandong, Liaoning Province, China. The chemical composition of the complex ore is shown in Table 1. It can be seen that the complex iron ore contains high contents of  $\text{MgO}$  and sulfur, however, the TFe and  $\text{B}_2\text{O}_3$  content are low. Mineralogical analysis of the concentrate is performed by X-ray diffraction (XRD). The result is given in Fig. 1, which indicates that

**Table 1** Chemical composition of ludwigite iron concentrate (mass fraction, %)

$\text{B}_2\text{O}_3$	TFe	$\text{MgO}$	$\text{SiO}_2$	$\text{Al}_2\text{O}_3$
6.90	47.20	19.20	5.32	0.15
FeO	CaO	P	S	LOI
18.90	0.34	0.020	0.16	4.97

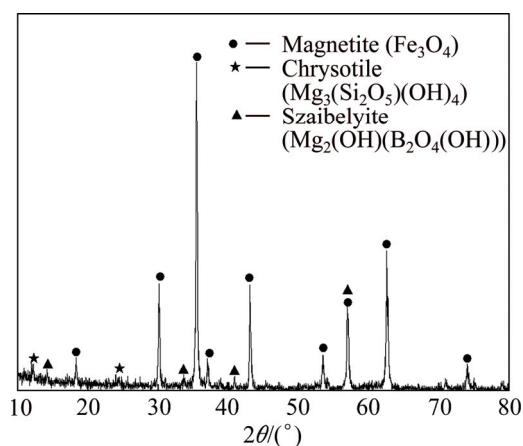


**Fig. 1** XRD pattern of ludwigite iron concentrate

the main crystalline phases are magnetite ( $\text{Fe}_3\text{O}_4$ ), szaibelyite ( $\text{Mg}_2(\text{OH})(\text{B}_2\text{O}_4(\text{OH}))$ ) and chrysotile ( $\text{Mg}_3(\text{Si}_2\text{O}_5)(\text{OH})_4$ ). The diameter of most particles (98%) of the iron ore concentrate is smaller than 0.074 mm. The SEM-EDS analysis of the concentrate is shown in Fig. 2 and Table 2, which reveal the complicated microstructure of the iron ore. Most of the magnetite particles are in isolated state and some of the magnetites conjunct with szaibelyite and chrysotile. Some of the chrysotile and szaibelyite particles also conjunct with each other. Small amount of  $\text{FeO}$  exists in the form of isomorphism with  $\text{MgO}$  in the minerals of szaibelyite and chrysotile. Based

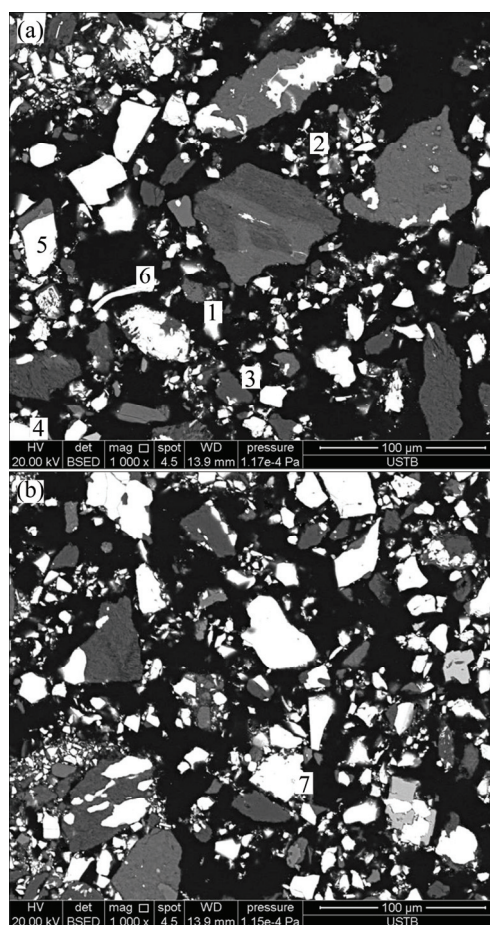


**Fig. 2** Microstructure images of ludwigite iron concentrate

**Table 2** EDS analysis of ludwigite iron concentrate

Position	Mass fraction/%							Mineral phase
	Fe	Mg	Si	Al	Ca	S	O	
1	3.36	29.84	18.94	—	—	—	47.86	Chrysotile
2	2.23	35.40	0.86	—	—	—	61.51	Szaibelyite
3	46.77	—	—	—	—	53.23	—	Pyrite
4	4.65	24.48	16.33	7.80	—	—	46.75	Chlorite
5	71.92	1.24	—	—	—	—	26.85	Magnetite
6	2.32	16.51	—	—	27.28	—	53.89	Dolomite
7	44.53	19.19	—	—	—	—	36.28	Ludwigite

on the EDS analysis result, it can be determined that the sulfur containing mineral in the ludwigite iron concentrate is pyrite ( $\text{FeS}_2$ ), and there are still some pyrrhotite ( $\text{Fe}_{1-x}\text{S}$ ) and chalcopyrite ( $\text{CuFeS}_2$ ) in little amount according to the literature reports [11].

The chemical composition of the reducing agent is listed in Table 3. It can be seen that the reducing agent is a kind of anthracite with high contents of fix carbon and low sulfur. The fineness of reducing agent is smaller than 0.5 mm. The reactivity of the pulverized coal is assessed by its chemical reaction rate with carbon dioxide (30 mL/min) by a thermogravimetric method with a heating rate of 10 °C/min. The result shows that the Boudouard reaction proceeds at viable rate when the temperature is higher than 1000 °C. The  $\text{Na}_2\text{CO}_3$  used in the experiment is of analytical reagent (AR) grade.

## 2.2 Experimental procedure

The ludwigite iron concentrate, reducing agent and  $\text{Na}_2\text{CO}_3$  were fully mixed together. The mole ratio of fixed carbon in reducing agent to oxygen of iron oxides in iron concentrate was 1.2. Nearly 70% of the total sulphur in the composite pellet was from the iron concentrate under the blending ratio. The mass of  $\text{Na}_2\text{CO}_3$  was set as 0, 2%, 4% and 6% of the total mass of iron concentrate and reducing agent. The moisture of the mixture was controlled as 7%. The mixture was pelletized in a horizontal twin roller machine. The size of the pillow shape pellet was 40 mm × 30 mm × 20 mm. The wet green pellets were dried for 12 h at 120 °C before reduction test.

Reduction and melting separation experiment was

performed in a closed  $\text{MoSi}_2$  box muffle resistance furnace to simulate the iron nugget production process of carbon composite pellet in the rotary hearth furnace. The schematic diagram of the experimental apparatus is shown in Fig. 3. In each experiment, the dry green pellet was put into a graphite crucible and then heated at temperatures of 1400 °C and 1450 °C in the furnace. The crucible had already been heated to the target temperature before the pellet was put into it. The graphite crucible would protect the furnace from being corroded by the formed slag. Once the reduction experiment was finished, the sample was taken out of the furnace and cooled to ambient temperature under the protection of nitrogen. The metallized pellets, which had not melted, were characterized by the index of metallization degree ( $\eta$ ). The  $\eta$  was calculated by the following formula:

$$\eta = w(\text{MFe})/w(\text{TFe}) \times 100\% \quad (1)$$

where  $w(\text{TFe})$  is the content of total iron after reduction,  $w(\text{MFe})$  is the content of metallic iron after reduction. The  $w(\text{TFe})$  and  $w(\text{MFe})$  of the pellet were obtained by chemical analysis.

The chemical composition of separated slag and iron nugget were analyzed to reveal the effect of  $\text{Na}_2\text{CO}_3$  addition on the melting separation behaviors. The XRD (for powder samples) and SEM-EDS (for polished blocky samples) analyses were also conducted aiming to characterize the phase composition and microstructure of the slag or reduced pellet. The melting temperature of slag was tested by so-called hemisphere method. The slag sample powder, whose particle size was less than 0.074 mm, was pressed into a column shape pellet with

**Table 3** Proximate and ash analysis results of reducing agent

Proximate analysis					Ash analysis				Ash fusibility			
$w(\text{FC}_d)/\%$	$w(\text{V}_d)/\%$	$w(\text{A}_d)/\%$	$w(\text{S})/\%$	$w(\text{SiO}_2)/\%$	$w(\text{Al}_2\text{O}_3)/\%$	$w(\text{Fe}_2\text{O}_3)/\%$	$w(\text{CaO})/\%$	$w(\text{MgO})/\%$	DT/°C	ST/°C	HT/°C	FT/°C
81.40	6.40	11.10	0.34	46.10	32.16	9.51	4.26	0.65	1300	1320	1350	1380

FC<sub>d</sub>: Fixed carbon (dry basis); V<sub>d</sub>: Volatile matter (dry basis); A<sub>d</sub>: Ash (dry basis); S: Total sulfur; DT: Deformation temperature; ST: Softening temperature; HT: Hemispherical temperature; FT: Flowing temperature

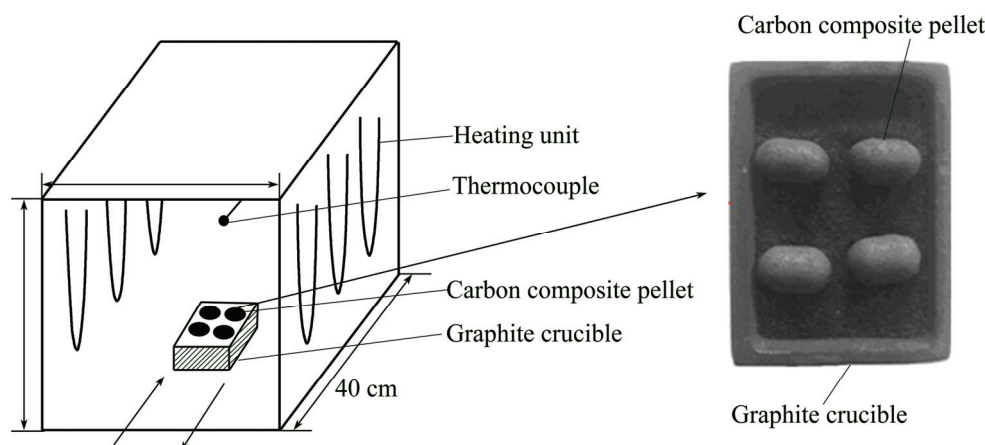


**Fig. 3** Schematic diagram of experimental apparatus



the size of  $d8 \text{ mm} \times 8 \text{ mm}$  and was heated in the furnace with the heating rate of  $10 \text{ }^\circ\text{C}/\text{min}$ . The melting point was defined as the temperature when the pellet shrinks into half of the initial height [12]. The value can help to understand the melting separation behavior of composite pellet. In order to assess the efficiency of extraction of boron (EEB) of the boron-rich slag, the normal pressure alkaline leaching method was applied. The parameters of the method were described as follows: mass of boron-rich slag: 4.000 g, particle size of slag: 98% less than  $0.074 \text{ mm}$ , concentration of lye: 20% NaOH, volume of lye: 40 mL, leaching time: 4 h. The boron content of primary and residual slag was analyzed by ICP-AES method. The EEB was defined by Eq. (2).

$$\text{EEB} = [(m_0 - m_1) / m_0] \times 100\% \quad (2)$$

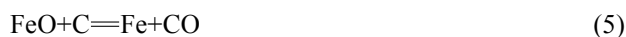
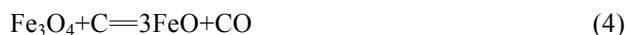
where  $m_0$  is the boron mass of primary slag,  $m_1$  is the boron mass of residual slag.

### 3 Results and discussion

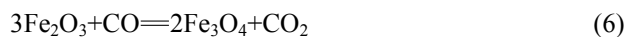
#### 3.1 Effect of $\text{Na}_2\text{CO}_3$ on reduction behaviors of composite pellet

The reduction behaviors of composite pellets containing 0, 2%, 4% and 6%  $\text{Na}_2\text{CO}_3$  at  $1400 \text{ }^\circ\text{C}$  are shown in Fig. 4. It can be seen that the metallization degree gradually increases with the increase of reduction time. The addition of  $\text{Na}_2\text{CO}_3$  can improve the reduction rate visibly. The reduction rates of the pellets containing  $\text{Na}_2\text{CO}_3$  are faster than that of the pellet without  $\text{Na}_2\text{CO}_3$ . It also can be seen that the reduction rates of the 4%  $\text{Na}_2\text{CO}_3$  and 6%  $\text{Na}_2\text{CO}_3$  pellets are both higher than that of the 2%  $\text{Na}_2\text{CO}_3$  pellet. During certain reduction stage, the reduction rates of 4%  $\text{Na}_2\text{CO}_3$  and 6%  $\text{Na}_2\text{CO}_3$  pellets are almost the same. The main reactions of iron oxide in the carbon composite pellet during reduction are as follows [8,13]:

Direct reductions



Indirect reductions



Boudouard reaction



At initial stage, the reduction reaction is dominated by the direct reduction due to the direct contact between iron oxide and coal and the absence of CO. With the

increase of temperature and CO pressure, the indirect reduction will dominate the total reduction reaction. The Boudouard reaction highly depends on the temperature and the  $\text{CO}_2$  produced from the indirect reduction will be consumed by the solid carbon through Boudouard reaction. At last, the total reduction reaction will abide by the formula  $\text{FeO}_x + x\text{C} = \text{Fe} + x\text{CO}$  through the gaseous intermediates CO and  $\text{CO}_2$ . It is believed that  $\text{Na}_2\text{CO}_3$  can catalyze the Boudouard reaction. Therefore, it will exert a positive influence on the reduction [14,15]. The catalysis effects of 4%  $\text{Na}_2\text{CO}_3$  and 6%  $\text{Na}_2\text{CO}_3$  do not differ much under the experimental condition.

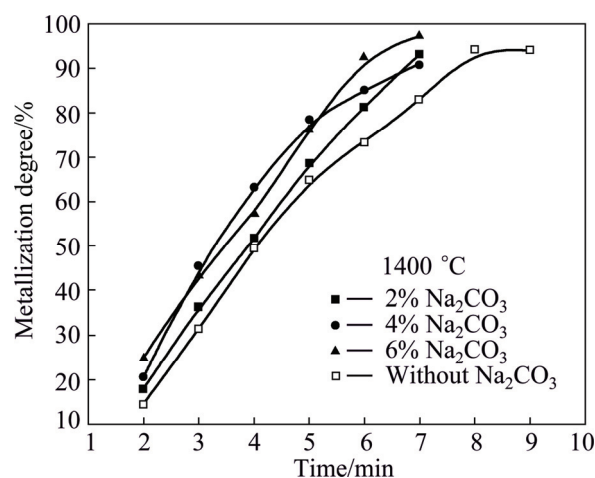


Fig. 4 Variation of metallization degree of composite pellet with different contents of  $\text{Na}_2\text{CO}_3$

During the reduction process, an interesting phenomenon occurs that the pellets containing  $\text{Na}_2\text{CO}_3$  will form lots of metallic iron particles on the surface of the reduced pellet when heated for a certain time. The iron particles gradually grow bigger with the reduction progressing. In the end, the samples, especially reduced for more than 7 min, cannot be milled into fine powders for chemical analysis. The morphology of the iron particles on the surface of the reduced 6%  $\text{Na}_2\text{CO}_3$  pellet is shown in Fig. 5.

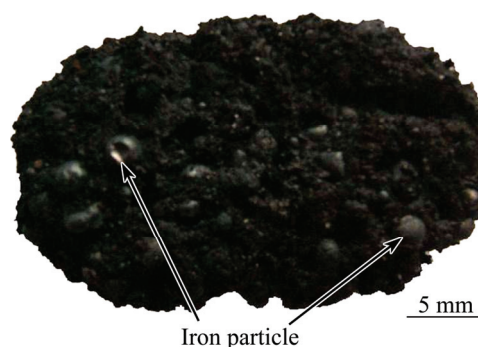


Fig. 5 Morphology of iron particles on surface of reduced pellets ( $1400 \text{ }^\circ\text{C}$ , 8 min, 6%  $\text{Na}_2\text{CO}_3$ )

### 3.2 SEM-EDS analysis of reduced pellets

Figure 6 shows the cross-sectional SEM images of the pellets containing different contents of  $\text{Na}_2\text{CO}_3$  reduced at 1400 °C for 7 min. The metallic iron and residual coal particles can be clearly seen in the image. The coal will be consumed during the reduction process and the diameter of the coal particle will then decrease forming the holes synchronously. The metallic iron usually gathers around the boundary of the coal particles, especially for the pellet without  $\text{Na}_2\text{CO}_3$ . The pellet bearing 2%  $\text{Na}_2\text{CO}_3$  has denser structure than others. More metallic iron particles will form in the gangue mineral phase for the pellet containing  $\text{Na}_2\text{CO}_3$  than the one without  $\text{Na}_2\text{CO}_3$ . The reason may be that the  $\text{Na}_2\text{CO}_3$  dissolves into the minerals of the iron ore and it will improve the reduction of the iron oxide topochemically. The porosity of the reduced pellet increases with the increase of  $\text{Na}_2\text{CO}_3$  content in the pellet. The diameter of the metallic iron particles of the reduced 6%  $\text{Na}_2\text{CO}_3$  pellet is the largest.

The mapping analysis of sulfur element is given in Fig. 7. It can be obviously seen that the sulfur concentrations in the metallic iron and coal particles are higher than that in the slag phase for all the sample pellets. It indicates that sulfur will be absorbed by newly formed metallic iron during the reduction process. Most of the sulfur in the composite pellet is in the form of

$\text{FeS}_2$ . When the heating temperature is around 500 °C,  $\text{FeS}_2$  will decompose through a disproportionation reaction, which is shown as Eq. (10):



Then, the elemental sulfur will volatilize into gas atmosphere. The elemental sulfur and FeS will react easily with CO to form COS if the CO partial pressure is very high and the COS will diffuse into the atmosphere [16,17].



Many researchers have obtained the similar conclusion that the desulfurization ratio through gaseous intermediates is less than 20% during the solid state reduction process of carbon composite pellet below the temperature of 1350 °C. Most of the sulfur in the pellet will still remain in the reduced pellet and the residual sulfur mainly gathers in the boundary between metallic iron and carbon particles [18,19]. Therefore, the desulfurization has to be realized by slag phase during the melting separation process.

### 3.3 Effect of $\text{Na}_2\text{CO}_3$ on melting separation behaviors of composite pellets

The morphologies of composite pellets containing

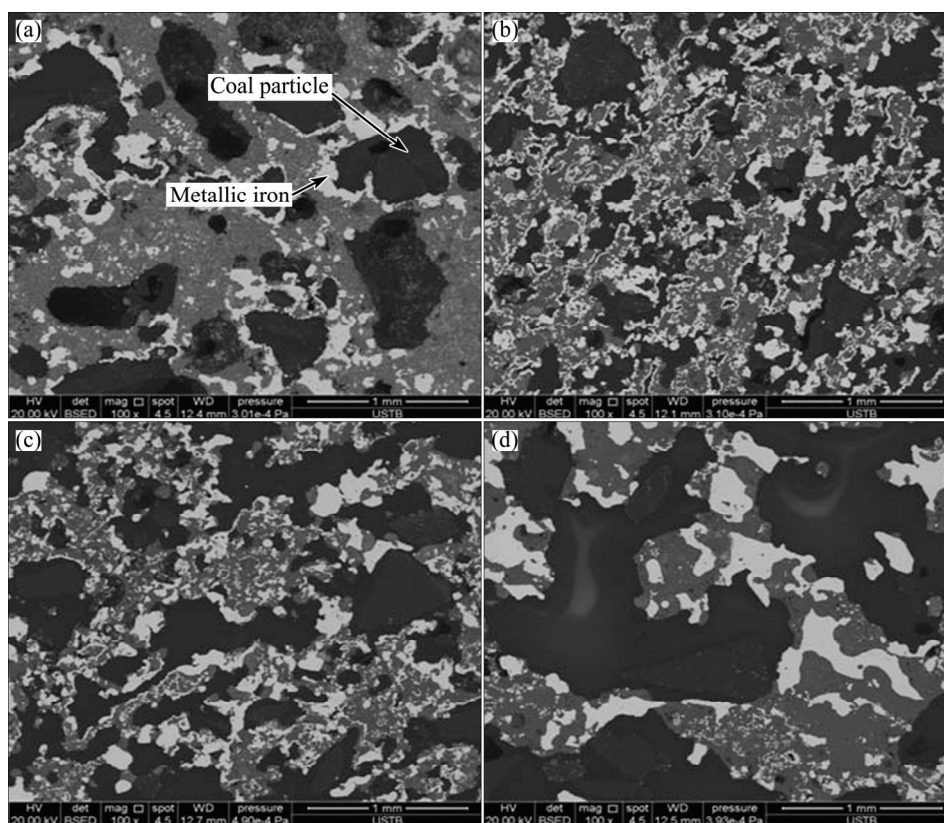


**Fig. 6** Microstructures of reduced pellets at 1400 °C for 7 min: (a) Without  $\text{Na}_2\text{CO}_3$ ; (b) 2%  $\text{Na}_2\text{CO}_3$ ; (c) 4%  $\text{Na}_2\text{CO}_3$ ; (d) 6%  $\text{Na}_2\text{CO}_3$



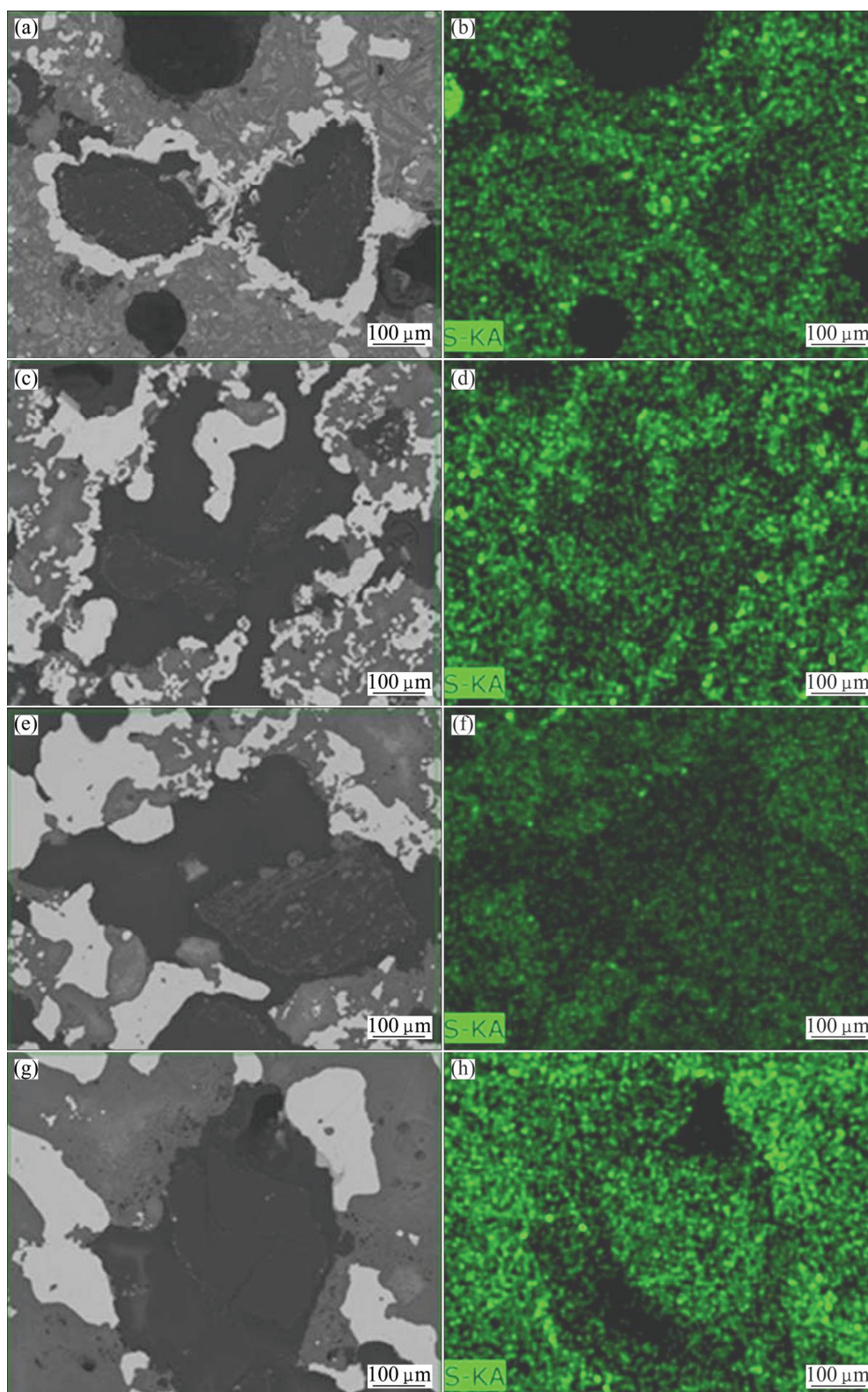


**Fig. 7** Mapping analysis of sulfur of reduced pellet: (a, b) Without  $\text{Na}_2\text{CO}_3$ ; (c, d) 2%  $\text{Na}_2\text{CO}_3$ ; (e, f) 4%  $\text{Na}_2\text{CO}_3$ ; (g, h) 6%  $\text{Na}_2\text{CO}_3$

$\text{Na}_2\text{CO}_3$  reduced at 1400 °C for 16 min are shown in Fig. 8. It can be seen that the added  $\text{Na}_2\text{CO}_3$  obviously affects the melting separation behaviors. For the 2%  $\text{Na}_2\text{CO}_3$  pellet, it begins to melt separation at 10 min and is nearly the same with the pellet without  $\text{Na}_2\text{CO}_3$ . However, the shapes of separated iron and slag are not

clean and there are many small iron particles around the boundary of slag. The melting separation manner becomes worse with the increase of  $\text{Na}_2\text{CO}_3$  in the pellet. The pellets containing 4%  $\text{Na}_2\text{CO}_3$  can only form smaller iron nugget at the boundary of slag. The pellets containing 6%  $\text{Na}_2\text{CO}_3$  cannot melt separation at all.

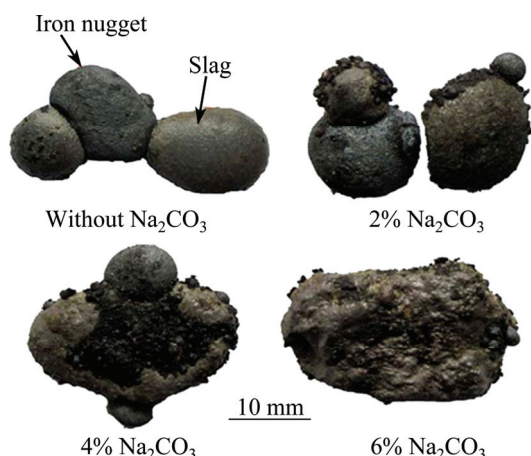


Fig. 8 Morphologies of reduced pellets (1400 °C, 16 min)

Generally speaking, the melting separation of the pellet can be improved if the reduction temperature is increased. The morphologies of composite pellets containing  $\text{Na}_2\text{CO}_3$  reduced at 1450 °C for 20 min are shown in Fig. 9. It can be observed that the pellet containing 6%  $\text{Na}_2\text{CO}_3$  still cannot separate well due to poor melting property of the slag. Chemical compositions of the slag separated from the pellets of 2%, 4% and 6%  $\text{Na}_2\text{CO}_3$  are given in Table 4. It shows that the FeO content in the slag is very low and nearly all the residual iron in the slag is in metallic form. The content of Na gradually increases. Based on mass balance calculation, nearly 61%, 62% and 57% of the total Na element were added into the 2%  $\text{Na}_2\text{CO}_3$ , 4%  $\text{Na}_2\text{CO}_3$  and 6%  $\text{Na}_2\text{CO}_3$  pellet volatile into gas atmosphere during the reduction and melting separation process, respectively. The melting point of  $\text{Na}_2\text{CO}_3$  is 850 °C and it will melt and decompose when the heating temperature

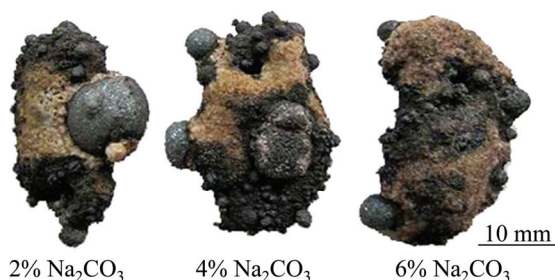
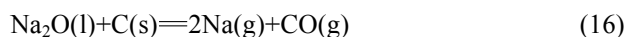
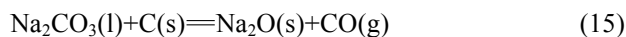
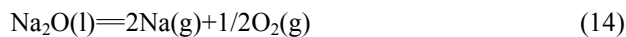
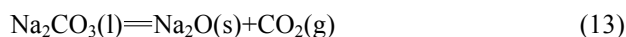


Fig. 9 Morphologies of reduced pellets (1450 °C, 20 min)

Table 4 Chemical composition of separated slags (mass fraction, %)

Slag	TFe	MFe	FeO	S	$\text{B}_2\text{O}_3$	Na
Without $\text{Na}_2\text{CO}_3$	5.74	4.08	2.13	0.12	20.01	0.12
2% $\text{Na}_2\text{CO}_3$	7.68	7.45	0.29	0.40	18.08	1.05
4% $\text{Na}_2\text{CO}_3$	6.01	5.56	0.58	0.48	16.60	2.01
6% $\text{Na}_2\text{CO}_3$	7.60	7.46	0.18	0.46	14.16	3.40

is higher than 850 °C, which are listed as Eqs. (13) and (14). The presence of solid carbon will highly improve the rate of decomposition of  $\text{Na}_2\text{CO}_3$  and the reactions are shown as Eqs. (15) and (16) [20].



The iron nugget formation process generally includes four typical stages (i.e., heating stage, reduction of iron ore, carburization of reduced iron, and melting separation of carburized iron and slag). Actually, the most important stages are the carburization and iron-slag melting separation. Many literatures reveal that the slag composition is related not only to its own melting, but also affects the carburization and consequently the melting separation of molten slag and iron-carbon alloy [21–24]. The melting points of the separated slag are shown in Fig. 10. It can be seen that the melting point of the slag increases heavily with the  $\text{Na}_2\text{CO}_3$  content increasing from 0 to 6%. The slag formed from the 6%  $\text{Na}_2\text{CO}_3$  pellet cannot melt down before 1470 °C. The effects of added  $\text{Na}_2\text{CO}_3$  on desulfurization and iron yield are shown in Fig. 11. The sulfur content of the iron nugget gradually decreases from 0.27% to 0.084% and the sulfur distribution ratio gradually increases, correspondingly. The sulfur content in the iron nugget separated from the pellet containing 6%  $\text{Na}_2\text{CO}_3$  is still a little higher for economical steel making. It should be refined for desulfurization or mixed with other low sulfur scrap in the further steel making. Addition of  $\text{Na}_2\text{CO}_3$  results in the melting difficulty and high viscosity of the slag at the experimental temperature. So, the metallic iron cannot aggregate sufficiently into large iron nugget and some small iron particles will remain in the slag. In the end, the yield of iron in the iron nugget form

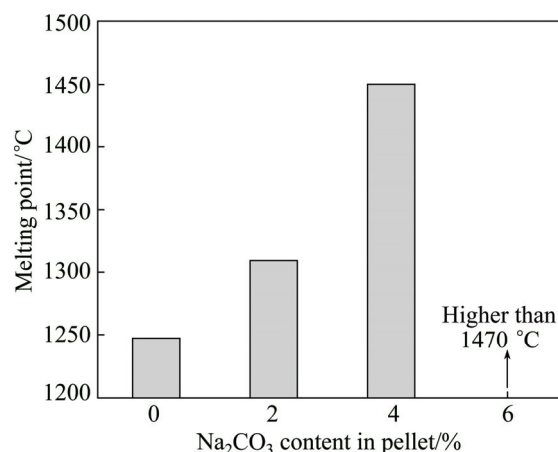
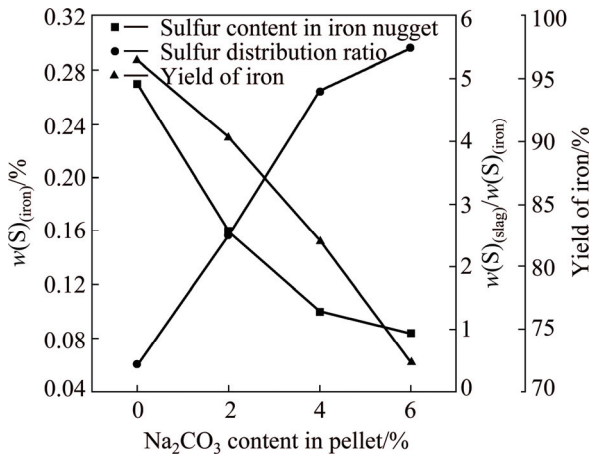


Fig. 10 Effect of  $\text{Na}_2\text{CO}_3$  addition on melting property of separated slag





**Fig. 11** Effect of Na<sub>2</sub>CO<sub>3</sub> addition on desulfurization and iron yield (1450 °C, 20 min)

decreases from 96.5% to 72.3% with the increase of Na<sub>2</sub>CO<sub>3</sub> content from 0 to 6%. The morphology of the residual metallic iron particles in the separated slag (6% Na<sub>2</sub>CO<sub>3</sub>) is shown in Fig. 12.

**3.4 Effect of Na<sub>2</sub>CO<sub>3</sub> on microstructure of slag phase**

The melting point of the boron-rich slag increases with the addition of Na<sub>2</sub>CO<sub>3</sub>, which results in the worse

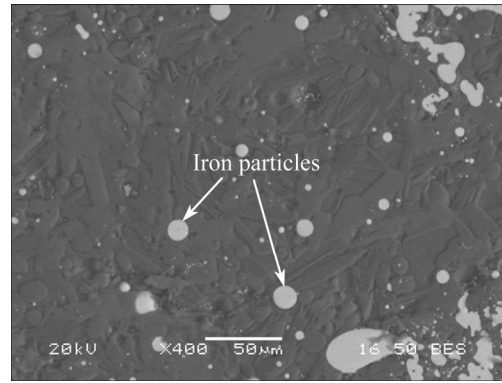


**Fig. 12** Morphology of residual metallic iron particles in separated slag (6% Na<sub>2</sub>CO<sub>3</sub>)

melting separation. All the experimental results indicate that the microstructure of the molten boron-rich slag has changed due to the presence of Na<sub>2</sub>CO<sub>3</sub>. The pellets bearing Na<sub>2</sub>CO<sub>3</sub> are reduced at 1450 °C for 20 min and then are quickly air quenched to room temperature. The mineral phase compositions of the quenched slag are investigated by XRD.

The XRD patterns of the quenched boron-rich slag are shown in Fig. 13. It can be obviously seen that the

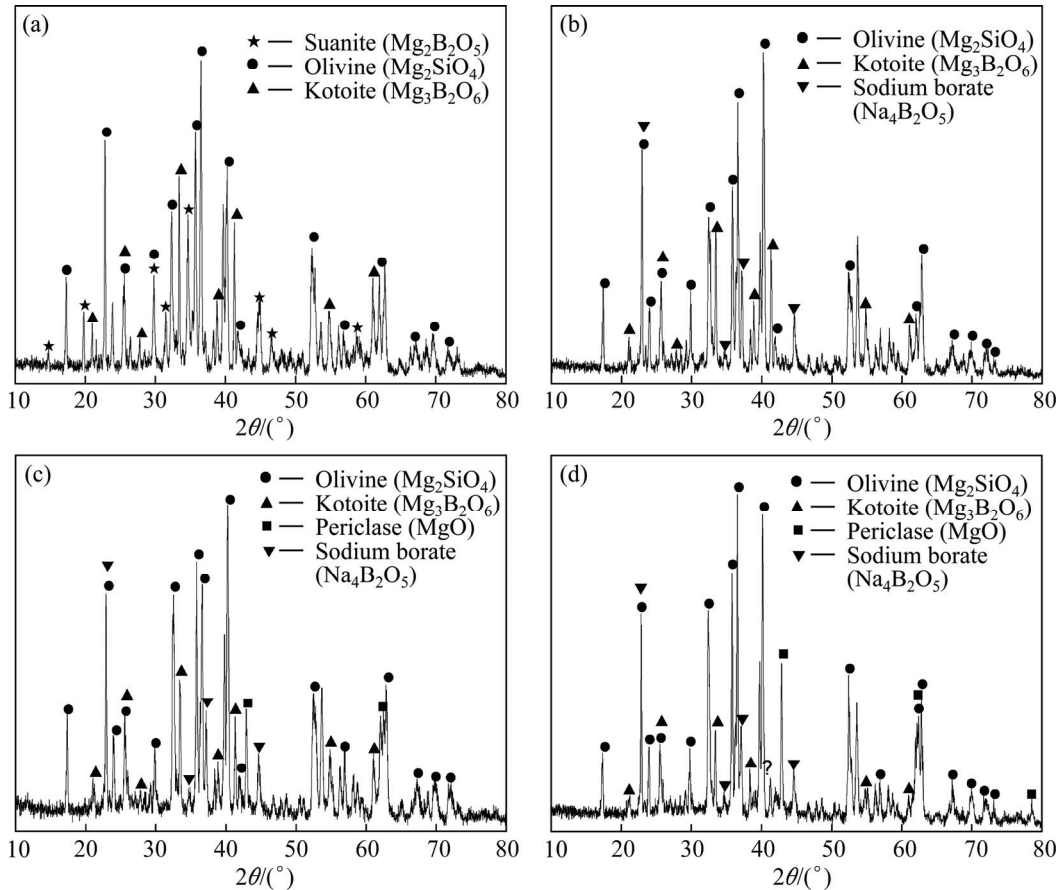


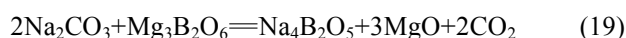
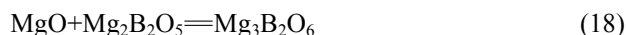
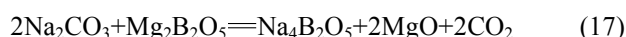
**Fig. 13** XRD patterns of separated boron-rich slag (1450 °C, 20 min, air quenched): (a) Without Na<sub>2</sub>CO<sub>3</sub>; (b) 2% Na<sub>2</sub>CO<sub>3</sub>; (c) 4% Na<sub>2</sub>CO<sub>3</sub>; (d) 6% Na<sub>2</sub>CO<sub>3</sub>



addition of  $\text{Na}_2\text{CO}_3$  has great influence on the mineral phase composition of the slag. For the slag separated from the pellet without  $\text{Na}_2\text{CO}_3$ , the main crystalline phases are olivine ( $\text{Mg}_2\text{SiO}_4$ ), kotoite ( $\text{Mg}_3\text{B}_2\text{O}_6$ ) and suanite ( $\text{Mg}_2\text{B}_2\text{O}_5$ ). For the slag separated from the 2%  $\text{Na}_2\text{CO}_3$  pellet, the main crystalline phases are olivine ( $\text{Mg}_2\text{SiO}_4$ ) and kotoite ( $\text{Mg}_3\text{B}_2\text{O}_6$ ) and sodium borate ( $\text{Na}_4\text{B}_2\text{O}_5$ ). The new phase sodium borate comes into being due to the addition of  $\text{Na}_2\text{CO}_3$ . The suanite phase disappears and the amount of kotoite decreases at the same time. For the slag separated from the 4%  $\text{Na}_2\text{CO}_3$  pellet, the main crystalline phases are olivine ( $\text{Mg}_2\text{SiO}_4$ ), kotoite ( $\text{Mg}_3\text{B}_2\text{O}_6$ ), sodium borate ( $\text{Na}_4\text{B}_2\text{O}_5$ ) and periclase ( $\text{MgO}$ ). The new phase periclase comes into being. The slag separated from 6%  $\text{Na}_2\text{CO}_3$  pellet has the same species of crystalline phases with the slag of 4%  $\text{Na}_2\text{CO}_3$  pellet and the content of periclase increases. Totally speaking, the amount of boron-containing crystalline phase (i.e., kotoite and suanite) gradually decreases with the increase of  $\text{Na}_2\text{CO}_3$  and forms the sodium borate. The precipitation of the periclase and the increase of its amount will increase the melting point of the slag, which makes the melting separation of the pellet become worse.

The addition of  $\text{Na}_2\text{CO}_3$  has negative influence on the crystallization of suanite and kotoite, and will improve the formation of sodium borate and periclase.

The possible reactions are listed as follows [25]:



At first step, the added  $\text{Na}_2\text{CO}_3$  may react with suanite forming  $\text{MgO}$  and  $\text{Na}_4\text{B}_2\text{O}_5$ . And then,  $\text{MgO}$  will react with suanite forming kotoite. Therefore, the amount of suanite has decreased sharply once the  $\text{Na}_2\text{CO}_3$  is added. With the further increase of the amount of  $\text{Na}_2\text{CO}_3$  in the pellet, the  $\text{Na}_2\text{CO}_3$  will then react with kotoite forming  $\text{MgO}$  and  $\text{Na}_4\text{B}_2\text{O}_5$ . So, the amount of kotoite will decrease and the amount of periclase will increase during the reduction and melting separation process of the pellet with the addition of  $\text{Na}_2\text{CO}_3$ . The formation of periclase and the further increase of its content will increase the melting point of the slag and the melting separation of the pellet will then become more difficult.

### 3.5 Property of separated boron-rich slag

The pellets containing 0, 2%, 4% and 6%  $\text{Na}_2\text{CO}_3$  are reduced and realize melting separation, and then shut down the furnace to make the slag cool slowly in the furnace. The XRD patterns of slow cooled boron-rich slag are shown in Fig. 14. For the slag separated from the pellet without  $\text{Na}_2\text{CO}_3$ , the crystalline phases are suanite,

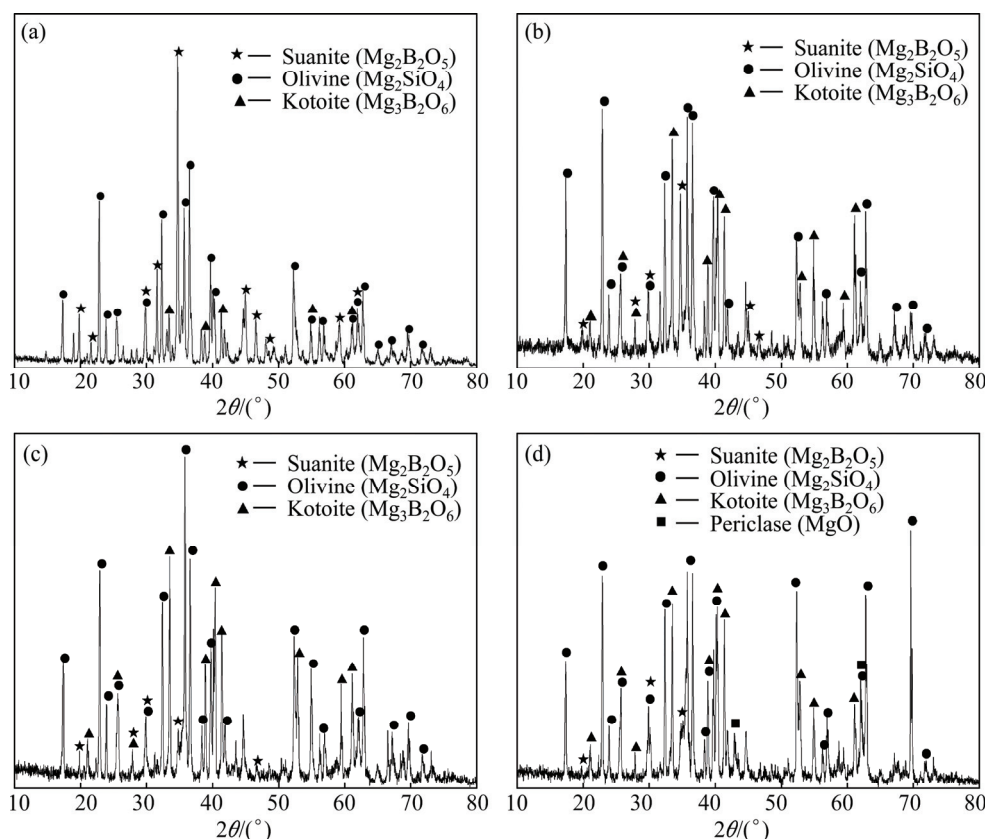


**Fig. 14** XRD patterns of slow cooled boron-rich slag (1450 °C, 20 min): (a) Without  $\text{Na}_2\text{CO}_3$ ; (b) 2%  $\text{Na}_2\text{CO}_3$ ; (c) 4%  $\text{Na}_2\text{CO}_3$ ; (d) 6%  $\text{Na}_2\text{CO}_3$

kotoite and olivine, and suanite is the main boron-containing crystalline phase. The slag separated from 2%  $\text{Na}_2\text{CO}_3$  pellet contains the same kinds of crystalline phases as that separated from the pellet without  $\text{Na}_2\text{CO}_3$ ; however, the peak of suanite decreases and the peak of kotoite increases. For the slag separated from the 4%  $\text{Na}_2\text{CO}_3$  pellet, the species of crystalline phases are the same as the 2%  $\text{Na}_2\text{CO}_3$  pellet separated slag. However, the peaks of suanite decrease and the peaks of olivine increase. It indicates that the amounts of boron-containing crystalline phases become less. For the slag separated from the 6%  $\text{Na}_2\text{CO}_3$  pellet, the main crystalline phases are kotoite, olivine, suanite and periclase. The new phase, periclase, forms in small quantities. The amounts of boron-containing crystalline phases in the slag keep the tendency of decreasing with the increase of added  $\text{Na}_2\text{CO}_3$ .

The SEM images and mapping analysis results of the slow cooled boron-rich slag separated from the pellet containing 6%  $\text{Na}_2\text{CO}_3$  are shown in Fig. 15 and Table 5, respectively. The main crystalline phases are olivine (phase 1) and kotoite (phase 2), which agrees well with the XRD analysis result. The  $\text{Na}_2\text{O}$  combines with  $\text{MgO}$ ,  $\text{SiO}_2$  and  $\text{Al}_2\text{O}_3$  forming a single phase (phase 3).

The EEB of the slow cooled boron-rich slag is shown in Fig. 16. The EEB closely depends on the

**Table 5** EDS analysis results of slow cooled boron-rich slag (6%  $\text{Na}_2\text{CO}_3$ , 1450 °C, 20 min)

Position	Mass fraction/%							Phase
	O	Mg	Al	Si	Na	Mn	Fe	
1	40.61	39.53	0.12	18.84	0.39	0.16	0.35	Olivine
2	48.58	49.93	0.04	0.44	0.64	0.15	0.22	Kotoite
3	43.95	18.84	15.22	9.81	11.87	0.17	0.14	Na-rich phase

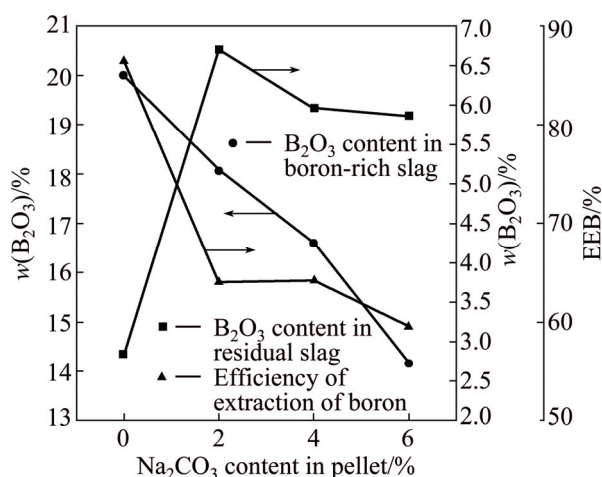


**Fig. 16** Extractive property of slow cooled boron-rich slag

species of boron containing crystalline phases and their amount. The chemical stability of kotoite is better than suanite and the EEB of suanite is better than kotoite [26]. The main boron containing crystalline phase in the slow cooled slag separated from the pellet without additive is suanite and its EEB is as high as 86.46%. All the EEB values of the slag separated from the pellet containing  $\text{Na}_2\text{CO}_3$  in the present study are lower than that. The EEB of the slag separated from the 2%  $\text{Na}_2\text{CO}_3$  pellet is nearly the same as that separated from the 4%  $\text{Na}_2\text{CO}_3$  pellet. The EEB of the slag decreases with the  $\text{Na}_2\text{CO}_3$  content in the pellet further increasing from 4% to 6% due to the decrease of total amount of boron-containing crystalline phases. Therefore, the addition of  $\text{Na}_2\text{CO}_3$  has obviously negative effect on the EEB of boron-rich slag under the present experimental condition.

## 4 Conclusions

1) The metallization degree of ludwigite/coal composite pellet increases with the increase of  $\text{Na}_2\text{CO}_3$  content in the pellet. Metallic iron particles will form on the surface of the pellet during the reduction process due to the addition of  $\text{Na}_2\text{CO}_3$ . The sulfur in the pellet will be absorbed by newly formed metallic iron during reduction process, which makes the desulfurization during the solid state stage very difficult.

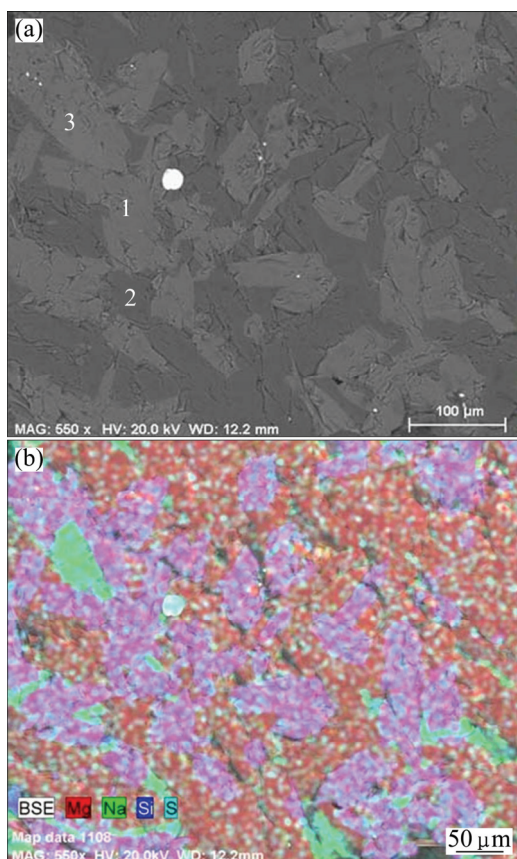


**Fig. 15** SEM image (a) and EDS mapping (b) of slow cooled boron-rich slag (6%  $\text{Na}_2\text{CO}_3$ , 1450 °C, 20 min)

2) The 2%  $\text{Na}_2\text{CO}_3$  composite pellet can melt separation when reduced at 1400 °C for 16 min. The pellets containing 4% and 6%  $\text{Na}_2\text{CO}_3$  cannot realize melt separation under the same condition, and melt partially when the heating temperature increases to 1450 °C because  $\text{Na}_2\text{CO}_3$  will heavily increase the melting point of the slag. Many small iron particles will form around the boundary of slag. The sulfur content of the iron nugget gradually decreases from 0.27% to 0.084% with the  $\text{Na}_2\text{CO}_3$  content in the pellet increasing from 0 to 6%. However, the yield of iron will decrease from 96.5% to 72.3% synchronously.

3)  $\text{Na}_2\text{CO}_3$  will improve the formation of kotoite instead of suanite when the  $\text{Na}_2\text{CO}_3$  content in the pellet is relatively low. The formed kotoite will react with  $\text{Na}_2\text{CO}_3$  forming  $\text{Na}_4\text{B}_2\text{O}_5$  and  $\text{MgO}$  with the further increase of  $\text{Na}_2\text{CO}_3$  content. So, the EEB of the boron-rich slag gradually decreases and the melting point of the slag gradually increases with the  $\text{Na}_2\text{CO}_3$  content in the pellet increasing from 0 to 6%.

## References

- [1] KEN S, MARCIA K M. Mineral commodity summaries [M]. Reston: U.S. Geological Survey, 2012.
- [2] ZHANG Xian-peng, LANG Jian-feng, CUI Chuan-meng, LIU Su-lan. Comprehensive utilization of low grade ludwigite ore with blast furnace smelting [J]. *Iron and Steel*, 1995, 30(12): 9–11. (in Chinese)
- [3] LIU Ran, XUE Xiang-xin, JIANG Tao, ZHANG Shu-hui, HUANG Da-wei. Comprehensive utilization of ludwigite and its prospect [J]. *Multipurpose Utilization of Mineral Resources*, 2006, (2): 33–37. (in Chinese)
- [4] LIU Su-lan, CUI Chuan-meng, ZHANG Xian-peng. Pyrometallurgical separation of boron from iron in ludwigite ore [J]. *ISIJ International*, 1998, 38(10): 1077–1079.
- [5] WANG Chang-ren, LIAN Xiang-quan. On some problems of the beneficiation of boron-iron ores [J]. *Metal Mine*, 1995, 24(9): 29–32. (in Chinese)
- [6] ZHAO Qing-jie. Separating iron from boric iron ore by selective reduction [J]. *Journal of Northeastern University*, 1990, 11(2): 122–126. (in Chinese)
- [7] WANG Guang, WANG Jing-song, DING Yin-gui, MA Sai, XUE Qing-guo. New separation method of boron and iron from ludwigite based on carbon bearing pellet reduction and melting technology [J]. *ISIJ International*, 2012, 52(1): 45–51.
- [8] WANG Guang, DING Yin-gui, WANG Jing-song, SHE Xue-feng, XUE Qing-guo. Effect of carbon species on the boron-bearing iron concentrate/carbon composite pellet reduction and melting behavior [J]. *International Journal of Minerals, Metallurgy and Materials*, 2013, 20(6): 522–528.
- [9] DING Yin-gui, WANG Jing-song, WANG Guang, MA Sai, XUE Qing-guo. Comprehensive utilization of paigeite ore using iron nugget process [J]. *Journal of Iron and Steel Research International*, 2012, 19(6): 9–13.
- [10] MORI K, WADA H, PEHLKE R D. Simultaneous desulfurization and dephosphorization reactions of molten iron by soda ash treatment [J]. *Metallurgical and Materials Transactions B*, 1985, 16(2): 303–312.
- [11] LI Yan-jun, GAO Tai, HAN Yue-xin. Research on processing mineralogy of paigeite [J]. *Non-Ferrous Mining and Metallurgy*, 2006, 22(6): 14–16. (in Chinese)
- [12] WANG Hong-ming, ZHANG Ting-wang, ZHU Hua, LI Gui-rong, YAN Yong-qi, WANG Jian-hua. Effect of  $\text{B}_2\text{O}_3$  on melting temperature, viscosity and desulfurization capacity of CaO-based refining flux [J]. *ISIJ International*, 2011, 51(5): 702–706.
- [13] YANG J, MORI T. Mechanism of carbothermic reduction of hematite in hematite-carbon composite pellets [J]. *ISIJ International*, 2007, 47(10): 1394–1400.
- [14] RAO Y K. Catalysis in extractive metallurgy [J]. *JOM*, 1983, 35(7): 46–50.
- [15] BASUMALLICK A. Influence of CaO and  $\text{Na}_2\text{CO}_3$  as additive on the reduction of hematite–lignite mixed pellets [J]. *ISIJ International*, 1995, 35(9): 1050–1053.
- [16] WU Xiao-dan, HU Hao-quan. Coal pyrolysis desulfurization in different atmosphere [J]. *Coal Conversion*, 2002, 25(4): 6–15. (in Chinese)
- [17] YI Ping-gui, YU Qing-sen, ZONG Han-xing. Thermodynamic analysis for chemical desulfurization of pyrite in coal [J]. *Coal Conversion*, 1999, 22(1): 47–52. (in Chinese)
- [18] INABA S, KIMURA Y. Behavior of sulfur in the carbon-bearing iron oxide pellet during heating [J]. *ISIJ International*, 2004, 44(12): 2112–2114.
- [19] DUAN Dong-ping, WAN Tian-ji, GUO Zhan-cheng. Decomposition and transformation behavior of sulfur in composite briquette/pellet of iron ore and coal [J]. *Journal of Iron and Steel Research*, 2005, 17(5): 16–21. (in Chinese)
- [20] KIM J W, LEE H G. Thermal and carbothermic decomposition of  $\text{Na}_2\text{CO}_3$  and  $\text{Li}_2\text{CO}_3$  [J]. *Metallurgical and Materials Transactions B*, 2001, 32(1): 17–24.
- [21] MATSUI T, ISHIWATA N, HARA Y, TAKEDA K. Influence of gangue composition on melting behavior of coal-reduced iron mixture [J]. *ISIJ International*, 2004, 44(12): 2105–2111.
- [22] SATOH K, NOGUCHI T, HINO M. Reduction and carburization of iron oxide by carbonaceous materials [J]. *Steel Research International*, 2010, 81(10): 834–840.
- [23] KIM H S, KIM J G, SASAKI Y. The role of molten slag in iron melting process for the direct contact carburization: Wetting and separation [J]. *ISIJ International*, 2010, 50(8): 1099–1106.
- [24] KIM H S, KANG Y B, KIM J G, SASAKI Y. The role of iron oxide bearing molten slag in iron melting process for the direct contact carburization [J]. *ISIJ International*, 2011, 51(1): 166–168.
- [25] LI Jie, FAN Zhan-guo. Study on influencing factors on preparing process of borax from boron-rich slag [J]. *Journal of Northeastern University*, 2009, 30(12): 1755–1758. (in Chinese)
- [26] ZHANG Pei-xin, SUI Zhi-tong. Effect of factors on the extraction of boron from slags [J]. *Metallurgical and Materials Transactions B*, 1995, 26(2): 345–351.



## Na<sub>2</sub>CO<sub>3</sub> 对硼铁矿含碳球团还原熔分行为及富硼渣性能的影响

王 广, 薛庆国, 王静松

北京科技大学 钢铁冶金新技术国家重点实验室, 北京 100083

**摘 要:** 在实验室条件下研究了 Na<sub>2</sub>CO<sub>3</sub> 对硼铁矿含碳球团还原熔分行为、脱硫率以及熔分富硼渣性能的影响。Na<sub>2</sub>CO<sub>3</sub> 在一定程度上可以提高硼铁矿含碳球团的还原速率。随着 Na<sub>2</sub>CO<sub>3</sub> 配比的增加, 含碳球团的熔分效果逐渐变差, 主要原因在于 Na<sub>2</sub>CO<sub>3</sub> 会显著提高富硼渣的熔点, 导致球团难以熔分。当球团中 Na<sub>2</sub>CO<sub>3</sub> 的质量分数从 0 增加至 6% 时, 球团中的硫含量(质量分数)逐渐从 0.27% 降低至 0.084%。与此同时, 缓冷富硼渣的萃取率从 86.46% 降低至 59.52%。实验结果表明, Na<sub>2</sub>CO<sub>3</sub> 的加入会对硼铁矿含碳球团的熔分效果和富硼渣中硼的提取产生不利影响。

**关键词:** 硼铁矿; 含碳球团; 还原熔分; 脱硫; 富硼渣; 提硼

(Edited by Yun-bin HE)